

Parallel MIC(0) Preconditioning for Numerical Upscaling of Anisotropic Linear Elastic Materials

S. Margenov and Y. Vutov

Institute for Parallel Processing

Abstract. Numerical homogenization is used for upscaling of the linear elasticity tensor of strongly heterogeneous microstructures. The implemented 3D algorithm is described in terms of six auxiliary elastic problems for the reference volume element (RVE). Rotated trilinear Rannacher-Turek finite elements are used for discretization of the involved subproblems. A parallel PCG method is implemented for efficient solution of the arising large-scale systems with sparse, symmetric, and positive semidefinite matrices. The implemented preconditioner is based on modified incomplete Cholesky factorization MIC(0).

The numerical homogenization scheme is derived on the assumption of periodic microstructure. This implies periodic boundary conditions (PBCs) on the RVE. From algorithmic point of view, an important part of this study concerns the incorporation of PBCs in the parallel MIC(0) solver.

Numerical upscaling results are shown. The test problem represents a trabecular bone tissue, taking into account the elastic response of the solid phase. The voxel microstructure of the bone is extracted from a high resolution computer tomography image. The presented results evidently demonstrate that the bone tissues could be substantially anisotropic.

The computations are performed on IBM Blue Gene/P machine at the Bulgarian Supercomputing Center.

1 Introduction

The Preconditioned Conjugate Gradient (PCG) method is known to be the best solution tool for large systems of linear equations with symmetric and positive definite sparse matrices [2]. The used preconditioning technique is crucial for the PCG performance. It is also known that the PCG method converges for semidefinite matrices in the orthogonal to the kernel subspace.

This paper is organized as follows. The applied numerical homogenization scheme is given in section 2. In section 3 the parallel MIC(0) preconditioner is described. Some results from numerical experiments are presented in the last section.

2 Homogenization Scheme

Let Ω be a hexahedral domain representing our RVE and $\mathbf{u} = (u_1, u_2, u_3)$ be the displacements in Ω . The components of the small strain tensor are:

$$\varepsilon_{ij}(\mathbf{u}(\mathbf{x})) = \frac{1}{2} \left(\frac{\partial u_i(\mathbf{x})}{\partial x_j} + \frac{\partial u_j(\mathbf{x})}{\partial x_i} \right) \quad (1)$$

We assume that the Hooke's law holds:

$$\sigma_{ij}(\mathbf{x}) = c_{ijkl}(\mathbf{x})\varepsilon_{kl}(\mathbf{x}) \quad (2)$$

Here, the Einstein summation convention is assumed. The tensor \mathbf{c} is called stiffness tensor and $\boldsymbol{\sigma}$ is the stress tensor. We can rewrite (2) in matrix notation

$$\begin{bmatrix} \sigma_{11} \\ \sigma_{22} \\ \sigma_{33} \\ \sigma_{23} \\ \sigma_{13} \\ \sigma_{12} \end{bmatrix} = \begin{bmatrix} c_{1111} & c_{1122} & c_{1133} & c_{1123} & c_{1113} & c_{1112} \\ c_{2211} & c_{2222} & c_{2233} & c_{2223} & c_{2213} & c_{2212} \\ c_{3311} & c_{3322} & c_{3333} & c_{3323} & c_{3313} & c_{3312} \\ c_{2311} & c_{2322} & c_{2333} & c_{2323} & c_{2313} & c_{2312} \\ c_{1311} & c_{1322} & c_{1333} & c_{1323} & c_{1313} & c_{1312} \\ c_{1211} & c_{1222} & c_{1233} & c_{1223} & c_{1213} & c_{1212} \end{bmatrix} \begin{bmatrix} \varepsilon_{11} \\ \varepsilon_{22} \\ \varepsilon_{33} \\ 2\varepsilon_{23} \\ 2\varepsilon_{13} \\ 2\varepsilon_{12} \end{bmatrix}. \quad (3)$$

The symmetric 6×6 matrix C is called stiffness matrix. For an isotropic materials C has only 2 independent degrees of freedom. For orthotropic materials (there are three orthogonal planes of symmetry in this case), the matrix C has 9 independent degrees of freedom — 3 Young's moduli E_1, E_2, E_3 , 3 Poisson's ratios $\nu_{23}, \nu_{31}, \nu_{12}$ and 3 shear moduli $\mu_{23}, \mu_{31}, \mu_{12}$.

$$C^{Ort} = \begin{bmatrix} \frac{1 - \nu_{23}\nu_{32}}{E_2 E_3 \Delta} & \frac{\nu_{21} + \nu_{31}\nu_{23}}{E_2 E_3 \Delta} & \frac{\nu_{31} + \nu_{21}\nu_{32}}{E_2 E_3 \Delta} \\ \frac{\nu_{12} + \nu_{13}\nu_{32}}{E_2 E_3 \Delta} & \frac{1 - \nu_{31}\nu_{13}}{E_2 E_3 \Delta} & \frac{\nu_{32} + \nu_{31}\nu_{12}}{E_2 E_3 \Delta} \\ \frac{E_3 E_1 \Delta}{\nu_{13} + \nu_{12}\nu_{23}} & \frac{E_3 E_1 \Delta}{\nu_{23} + \nu_{13}\nu_{21}} & \frac{E_3 E_1 \Delta}{1 - \nu_{12}\nu_{21}} \\ \frac{E_1 E_2 \Delta}{E_1 E_2 \Delta} & \frac{E_1 E_2 \Delta}{E_1 E_2 \Delta} & \frac{E_1 E_2 \Delta}{E_1 E_2 \Delta} \\ & \mu_{23} & \\ & & \mu_{31} \\ & & & \mu_{12} \end{bmatrix}, \quad (4)$$

where $\Delta = \frac{1 - \nu_{12}\nu_{21} - \nu_{13}\nu_{31} - \nu_{23}\nu_{32} - 2\nu_{12}\nu_{23}\nu_{31}}{E_1 E_2 E_3}$, $\frac{\nu_{12}}{E_1} = \frac{\nu_{21}}{E_2}$, $\frac{\nu_{23}}{E_2} = \frac{\nu_{32}}{E_3}$, $\frac{\nu_{31}}{E_3} = \frac{\nu_{13}}{E_1}$.

We follow the numerical upscaling method from [4], see also [5]. The homogenization scheme requires to find the functions $\boldsymbol{\xi}^{kl} = (\xi_1^{kl}, \xi_2^{kl}, \xi_3^{kl})$, $k, l = 1, 2, 3$, satisfying the following problem in a weak formulation:

$$\int_{\Omega} \left(c_{ijpq}(x) \frac{\partial \xi_p^{kl}}{\partial x_q} \right) \frac{\partial \phi_i}{\partial x_j} d\Omega = \int_{\Omega} c_{ijkl}(x) \frac{\partial \phi_i}{\partial x_j} d\Omega, \quad \forall \phi \in \mathbf{H}_P^1(\Omega), \quad (5)$$

where $\boldsymbol{\phi} = \{\phi_i\}_{i=1}^3$ and $\mathbf{H}_P^1(\Omega) = \{\boldsymbol{\phi} \in \mathbf{H}^1 : \phi_i \text{ are } \Omega\text{-periodic}\}$. After computing the characteristic displacements $\boldsymbol{\xi}^{kl}$, we find the homogenized elasticity tensor \mathbf{c}^H using the explicit formula:

$$c_{ijkl}^H = \frac{1}{|\Omega|} \int_{\Omega} \left(c_{ijkl}(x) - c_{ijpq}(x) \frac{\partial \xi_p^{kl}}{\partial x_q} \right) d\Omega. \quad (6)$$

Due to the symmetry of the stiffness tensor \mathbf{c} , the following relations $\xi^{kl} = \xi^{lk}$ hold. Therefore, it is enough to solve six problems (5) to get the homogenized elasticity tensor.

Rotated trilinear (Rannacher-Turek) finite elements [11] are used for numerical solution of (5). This choice is motivated by the additional stability of the nonconforming FEM discretization in the case of strongly heterogeneous materials [1]. The construction of robust non-conforming FEM methods are generally based on application of mixed formulation leading to a saddle-point system. By the choice of non continuous finite elements for the dual (pressure) variable, it can be eliminated at the (macro)element level, and we get a symmetric positive (semi-)definite FEM system in primal (displacements) variables. We use this approach which is referred as *reduced and selective integration* (RSI) [8].

3 Parallel MIC(0) Preconditioning

Our preconditioning algorithm is based on a preexisting parallel MIC(0) elasticity solver [10], based on a parallel MIC(0) solver for symmetric and positive definite scalar elliptic problems [9]. The preconditioner uses the isotropic variant of the displacement decomposition (DD) method (see, e.g., [12]). We write the DD auxiliary matrix in the form

$$C_{DD} = \begin{bmatrix} A & & \\ & A & \\ & & A \end{bmatrix} \quad (7)$$

where A is the stiffness matrix corresponding to the bilinear form

$$a(u^h, v^h) = \int_{\Omega} E(\mathbf{x}) \left(\sum_{i=1}^3 \frac{\partial u}{\partial x_i} \frac{\partial v}{\partial x_i} \right) d\mathbf{x}, \quad (8)$$

where u and v are Ω -periodic functions. The DD splitting is motivated by the second Korn's inequality, which holds for the RSI FEM discretization under consideration.

A brief introduction to the modified incomplete factorization [13] is given below. Let us rewrite the real $N \times N$ matrix $A = (a_{ij})$ in the form

$$A = D - L - L^T$$

where D is the diagonal and $(-L)$ is the strictly lower triangular part of A . Then we consider the approximate factorization of A which has the form:

$$C_{MIC(0)} = (X - L)X^{-1}(X - L)^T \quad (9)$$

with $X = \text{diag}(x_1, \dots, x_N)$ being the diagonal matrix determined by the condition of equal rowsums. We are interested in the case when $X > 0$ and thus $C_{MIC(0)}$ is positive definite for the purpose of preconditioning. If this holds, we speak about *stable* MIC(0) factorization. Concerning the stability of MIC(0), the following theorem holds.

Theorem 1. *Let $A = (a_{ij})$ be a symmetric real $N \times N$ matrix and let $A = D - L - L^T$ be the splitting of A . Let us assume that*

$$\begin{aligned} L &\geq 0, \\ Ae &\geq 0, \\ Ae + L^T e &> 0, \quad e = (1, \dots, 1)^T \in R^N, \end{aligned} \quad (10)$$

i.e. that A is a weakly diagonally dominant with nonpositive offdiagonal entries and that $A + L^T = D - L$ is strictly diagonally dominant. Then the relation

$$x_i = a_{ii} - \sum_{k=1}^{i-1} \frac{a_{ik}}{x_k} \sum_{j=k+1}^N a_{kj} > 0$$

holds and the diagonal matrix $X = \text{diag}(x_1, \dots, x_N)$ defines stable MIC(0) factorization of A .

The perturbed version of MIC(0) algorithm is used in our study. This means that the incomplete factorization is applied to the matrix $\tilde{A} = A + \tilde{D}$. The diagonal perturbation $\tilde{D} = \tilde{D}(\xi) = \text{diag}(\tilde{d}_1, \dots, \tilde{d}_N)$ is defined as follows:

$$\tilde{d}_i = \begin{cases} \xi a_{ii} & \text{if } a_{ii} \geq 2w_i \\ \xi^{1/2} a_{ii} & \text{if } a_{ii} < 2w_i \end{cases}$$

where $0 < \xi < 1$ is a properly chosen parameter, and $w_i = \sum_{j>i} -a_{ij}$. In particular, this allows us to satisfy the stability conditions (10) in the case of PBCs.

The idea of our parallel algorithm is to apply the MIC(0) factorization on an auxiliary matrix B , which approximates A . The matrix B has a special block structure, which allows a scalable parallel implementation. Following the standard FEM assembling procedure we write A in the form $A = \sum_{e \in \omega_h} L_e^T A_e L_e$, where A_e is the element stiffness matrix, L_e stands for the restriction mapping of the global vector of unknowns to the local one, corresponding to the current element e . Let us consider the following approximation B_e of A_e :

$$A_e = \begin{bmatrix} a_{11} & a_{12} & a_{13} & a_{14} & a_{15} & a_{16} \\ a_{21} & a_{22} & a_{23} & a_{24} & a_{25} & a_{26} \\ a_{31} & a_{32} & a_{33} & a_{34} & a_{35} & a_{36} \\ a_{41} & a_{42} & a_{43} & a_{44} & a_{45} & a_{46} \\ a_{51} & a_{52} & a_{53} & a_{54} & a_{55} & a_{56} \\ a_{61} & a_{62} & a_{63} & a_{64} & a_{65} & a_{66} \end{bmatrix}, \quad B_e = \begin{bmatrix} b_{11} & a_{12} & a_{13} & a_{14} & a_{15} & a_{16} \\ a_{21} & b_{22} & a_{23} & a_{24} & a_{25} & a_{26} \\ a_{31} & a_{32} & b_{33} & 0 & 0 & 0 \\ a_{41} & a_{42} & 0 & b_{44} & 0 & 0 \\ a_{51} & a_{52} & 0 & 0 & b_{55} & 0 \\ a_{61} & a_{62} & 0 & 0 & 0 & b_{66} \end{bmatrix}.$$

The local numbering follows the pairs of the opposite nodes of the reference element. The diagonal entries of B_e are modified to hold the rowsum criteria. Assembling the locally defined matrices B_e we get the global matrix $B = \sum_{e \in \omega_h} L_e^T B_e L_e$. The condition number estimate $\kappa(B^{-1}A) \leq 3$ holds uniformly with respect to mesh parameter and possible coefficient jumps (see for the related analysis in [9]). The modified matrix B has diagonal blocks, corresponding to the (x, y) cross sections. This allows to perform in parallel the solution of linear systems with matrix (9) [9]. It is important to note that the PBCs do not change the diagonal blocks of the stiffness matrix A as well as of the auxiliary matrix B . However, there are changes in the structure of the offdiagonal blocks, which require some principal modifications in the parallel code. Finally, the implemented parallel preconditioner for the considered linear elasticity nonconforming FEM systems has the form:

$$C_{DD \text{ MIC}(0)} = \begin{bmatrix} C_{\text{MIC}(0)}(B) & & \\ & C_{\text{MIC}(0)}(B) & \\ & & C_{\text{MIC}(0)}(B) \end{bmatrix}.$$

4 Numerical Experiments

The analyzed test specimen is a part of trabecular bone tissue extracted from a high resolution computer tomography image [6]. The trabecular bone has a strongly expressed heterogeneous microstructure composed of solid and fluid phases. To get a periodic RVE, the specimen is mirrored three times, see Fig. 1. In

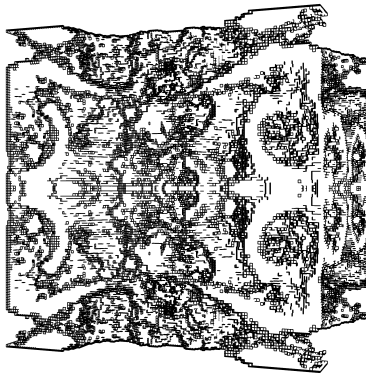


Fig. 1. Structure of the solid phase: $128 \times 128 \times 128$ voxels.

this article, our goal is to obtain the homogenized elasticity tensor of the trabecular bone tissue, taking into account the elastic response of the solid phase only.

To this purpose, numerical experiments with exponentially decreasing Young modulus for the voxels corresponding to the fluid phase are performed. In other words, the empty (fluid) voxels are interpreted as *fictitious domain*. Homogenized properties of different RVEs with varying size of $32 \times 32 \times 32$, $64 \times 64 \times 64$ and $128 \times 128 \times 128$ voxels are studied. The Young modulus and the Poisson ratio of the solid phase are taken from [3] as follows: $E^s = 14.7\text{GPa}$ and $\nu^s = 0.325$. We set also $\nu^f = \nu^s$ which practically doesn't influence the numerical upscaling results. In what follows, the fictitious domain Young modulus E^f is given in Pascals (see, e.g., the values in the parentheses bellow).

$$C^H[1.47 \times 10^7] = \begin{bmatrix} 4.86 \times 10^8 & 7.49 \times 10^7 & 6.74 \times 10^7 & & & \\ 7.49 \times 10^7 & 3.03 \times 10^8 & 9.45 \times 10^7 & & & \\ 6.74 \times 10^7 & 9.45 \times 10^7 & 7.43 \times 10^8 & & & \\ & & & 8.45 \times 10^7 & & \\ & & & & 6.22 \times 10^7 & \\ & & & & & 3.37 \times 10^7 \end{bmatrix}$$

$$C^H[1.47 \times 10^6] = \begin{bmatrix} 4.35 \times 10^8 & 5.65 \times 10^7 & 5.03 \times 10^7 & & & \\ 5.65 \times 10^7 & 2.38 \times 10^8 & 7.69 \times 10^7 & & & \\ 5.03 \times 10^7 & 7.69 \times 10^7 & 7.06 \times 10^8 & & & \\ & & & 6.66 \times 10^7 & & \\ & & & & 4.89 \times 10^7 & \\ & & & & & 1.40 \times 10^7 \end{bmatrix}$$

$$C^H[1.47 \times 10^5] = \begin{bmatrix} 4.29 \times 10^8 & 5.46 \times 10^7 & 4.86 \times 10^7 & & & \\ 5.46 \times 10^7 & 2.30 \times 10^8 & 7.49 \times 10^7 & & & \\ 4.86 \times 10^7 & 7.49 \times 10^7 & 7.01 \times 10^8 & & & \\ & & & 6.44 \times 10^7 & & \\ & & & & 4.74 \times 10^7 & \\ & & & & & 1.18 \times 10^7 \end{bmatrix}$$

Here we have vanished the entries of C^H which tend to zero with the increase of the PCG accuracy. The structure of C^H corresponds to the case of orthotropic materials which is due to the enforced triple mirroring procedure. Following (4), the Young moduli E_i in each of the coordinate directions and the Poisson ratios $\nu_{ij} = -\varepsilon_j/\varepsilon_i$ are computed explicitly by the formulas

$$E_i = 1/s_{ii} \quad \nu_{ij} = -E_i s_{ji}$$

where s_{ij} stand for the elements of the matrix $S = (C^H)^{-1}$, see [7].

Tables 1, 2 and 3 contain the computed homogenized Young moduli and Poisson ratios varying the fictitious domain Young modulus E^f for the considered three different specimens. A stable behaviour of the implemented numerical homogenization scheme is observed in all cases. From practical point of view, a good accuracy of the computed homogenized Young moduli and Poisson ratios is achieved if the fictitious domain modulus $E^f = \delta E^s$ for $\delta \in \{10^{-3}, 10^{-4}\}$. The next observation is that in all three cases (RVEs composed of 32^3 , 64^3 and

Table 1. Homogenized linear elasticity coefficients: $n=32$

E^f	E_1	E_2	E_3	ν_{12}	ν_{23}	ν_{31}	μ_{23}	μ_{31}	μ_{12}
1.47×10^9	4.52×10^9	6.23×10^9	6.24×10^9	0.208	0.300	0.286	2.29×10^9	1.39×10^9	1.35×10^9
1.47×10^8	2.03×10^9	4.72×10^9	4.67×10^9	0.095	0.271	0.229	1.73×10^9	4.81×10^8	3.80×10^8
1.47×10^7	1.67×10^9	4.48×10^9	4.45×10^9	0.074	0.264	0.212	1.66×10^9	3.56×10^8	2.42×10^8
1.47×10^6	1.63×10^9	4.46×10^9	4.42×10^9	0.072	0.263	0.210	1.65×10^9	3.42×10^8	2.26×10^8
1.47×10^5	1.62×10^9	4.45×10^9	4.42×10^9	0.071	0.262	0.210	1.65×10^9	3.40×10^8	2.24×10^8

Table 2. Homogenized linear elasticity coefficients: $n=64$

E^f	E_1	E_2	E_3	ν_{12}	ν_{23}	ν_{31}	μ_{23}	μ_{31}	μ_{12}
1.47×10^9	2.86×10^9	3.11×10^9	3.55×10^9	0.288	0.270	0.281	1.19×10^9	9.07×10^8	9.50×10^8
1.47×10^8	8.73×10^8	1.12×10^9	1.94×10^9	0.191	0.164	0.185	4.94×10^8	1.62×10^8	1.71×10^8
1.47×10^7	5.69×10^8	8.02×10^8	1.73×10^9	0.127	0.124	0.117	3.90×10^8	5.22×10^7	5.22×10^7
1.47×10^6	5.33×10^8	7.62×10^8	1.71×10^9	0.117	0.119	0.102	3.77×10^8	3.88×10^7	3.77×10^7
1.47×10^5	5.29×10^8	7.58×10^8	1.71×10^9	0.116	0.118	0.101	3.76×10^8	3.74×10^7	3.62×10^7

128^3 voxels) the orthotropy ratio is more than 3. This evidently confirms that the hypothesis that the trabecular bone structure could be interpreted (approximated) as isotropic is not realistic. The last table illustrates the convergence

Table 3. Homogenized linear elasticity coefficients: $n=128$

E^f	E_1	E_2	E_3	ν_{12}	ν_{23}	ν_{31}	μ_{23}	μ_{31}	μ_{12}
1.47×10^9	2.66×10^9	2.47×10^9	2.67×10^9	0.315	0.284	0.278	8.76×10^8	8.78×10^8	8.87×10^8
1.47×10^8	7.90×10^8	5.97×10^8	9.51×10^8	0.282	0.180	0.171	1.93×10^8	1.68×10^8	1.64×10^8
1.47×10^7	4.65×10^8	2.81×10^8	7.10×10^8	0.228	0.114	0.094	8.46×10^7	6.22×10^7	3.37×10^7
1.47×10^6	4.20×10^8	2.24×10^8	6.78×10^8	0.222	0.100	0.076	6.66×10^7	4.89×10^7	1.40×10^7
1.47×10^5	4.15×10^8	2.16×10^8	6.75×10^8	0.222	0.098	0.073	6.44×10^7	4.75×10^7	1.18×10^7

rate of the implemented DD MIC(0) preconditioner. The available theoretical estimates concern some more model problems for homogeneous materials. In such cases, the number of iterations is $n_{it} = O(n^{1/2}) = O(N^{1/6})$. Here the number of iterations has very similar behaviour for coefficient jumps of the range $\{10 - 10^2\}$. The good news here is that even for very large jumps of up to 10^5 , the convergence is only slightly deteriorating.

Based on the reported results we can conclude that the developed numerical homogenization algorithmis and software tools provide a reliable tool for computer simulation of strongly heterogeneous anisotropic voxel microstructure. As a next important step we plan to incorporate in the upscaling scheme the contribution of the fluid phase of the bone tissues. The implementation of additionally

Table 4. Number of iterations

n	E^f [Pa] N	1.47×10^9	1.47×10^8	1.47×10^7	1.47×10^6	1.47×10^5
32	2 359 296	222	363	575	711	734
64	18 874 368	343	577	848	1 236	1 436
128	150 994 944	481	840	1 505	2 311	2 482

stabilized solvers for PBC FEM problems as well as the incorporation of scalable AMG preconditioners in the composed algorithm are also under development.

5 Acknowledgments

The authors gratefully acknowledge the partial support provided via Bulgarian NSF Grant DO 02-147/08.

References

1. D.N. Arnold, F. Brezzi, Mixed and nonconforming finite element methods: Implementation, postprocessing and error estimates, *RAIRO, Model. Math. Anal. Numer.*,19 (1985), 7-32.
2. O. Axelsson, *Iterative Solution Methods*, Cambridge University Press, 1994.
3. S. Cowin, *Bone poroelasticity*, J. Biomechanics, **32** (1999), 217-238.
4. R. H.W. Hoppe and S. I. Petrova, *Optimal shape design in biomimetics based on homogenization and adaptivity*, Math. Comput. Simul., **65**(2004), No.3, 257-272.
5. A. Bensoussan, *Asymptotic Analysis for Periodic Structures*, Elsevier, Amsterdam, 1978.
6. Gisela Beller, Markus Burkhart, Dieter Felsenberg, Wolfgang Gowin, Hans-Christian Hege, Bruno Koller, Steffen Prohaska, Peter I. Sapiro and Jesper S. Thomsen: Vertebral Body Data Set ESA29-99-L3, <http://bone3d.zib.de/data/2005/ESA29-99-L3/>
7. M. H. Saad, *Elasticity - Theory, Applications and Numerics*, Elsevier, 2005.
8. D. Malkus, T. Hughes. Mixed finite element methods. Reduced and selective integration techniques: an uniform concepts. *Comp. Meth. Appl. Mech. Eng.*,15: 63-81, 1978.
9. P. Arbenz, S. Margenov, Y. Vutov, Parallel MIC(0) preconditioning of 3D elliptic problems discretized by Rannacher-Turek finite elements, *Computers and Mathematics with Applications*, 55 (10) (2008), 2197-2211.
10. Yavor Vutov, Parallel DD-MIC(0) Preconditioning of Nonconforming Rotated Trilinear FEM Elasticity Systems, *Large-Scale Scientific Computing*, Springer LNCS 4818 (2008), 745-752.
11. R. Rannacher, S. Turek, *Simple nonconforming quadrilateral Stokes Element*, Num. Meth. Part. Diff. Equs 8(2) (1992), 97-112.
12. R. Blaheta, *Displacement decomposition - incomplete factorization preconditioning techniques for linear elasticity problems*, Num. Lin. Algebr. Appl. 1 (1994), 107-126.
13. I. Gustafsson, *Modified incomplete Cholesky (MIC) factorization*, In: D.J. Evans (ed.): *Preconditioning Methods; Theory and Applications*, Gordon and Breach, 1983, 265-293.